ELSEVIER

Polymer 43 (2002) 4947–4955

polymer

www.elsevier.com/locate/polymer

Determination of the influence of the polymer structure and particle size on the film formation process of polymers by atomic force microscopy

Martina Meincken, Ronald D. Sanderson*

[a]*Department of Chemistry, Division of Polymer Science, University of Stellenbosch, Private Bag X1, Matieland 7602, South Africa*

Received 28 February 2002; received in revised form 27 May 2002; accepted 31 May 2002

Abstract

The particle size and morphology of a synthetic polymer latex were shown to influence the film formation behavior. Theoretical models predict that small particles coalesce more easily than large colloids do.

The influence of particle size and morphology of differently structured lattices on the film-formation process was investigated by atomic force microscopy (AFM). Sequences of AFM images were acquired over a certain temperature range or at room temperature as a function of time. From the resulting images the average particle diameter of the latex particles in the surface layer was determined as a function of the time or temperature. The resulting curves could be compared to observe differences in the film formation kinetics of the different lattices. These AFM studies confirmed that the film formation behavior is influenced by the particle size and particle morphology, but that the core/shell ratio of core–shell particles has no significant influence on the film formation kinetics.

Keywords: Atomic force microscopy; Film-formation; Latex

1. Introduction

One of the most important characteristics of latex particles used in coatings is their film formation or coalescence behavior that affects the properties of the resulting coating. A better understanding of the fundamental mechanism of film formation is important for the design of optimal coating systems. For a latex emulsion to form a smooth, continuous film under ambient conditions, the latex particles must be soft enough to deform and possibly interdiffuse. The glass transition temperature (T_g) is the temperature at which chain segments begin to move and molecules can interdiffuse. Thus, T_g is a particularly useful parameter to describe a polymer's ability to form a film.

A common way to manipulate the T_g of a latex is by the addition of coalescent aids or plasticizers, which lower the T_g of the latex in its wet state and allow film formation at a lower temperature. As the film dries, the solvents evaporate and leave a high T_g film, which is fairly stable.

A possible way to minimize the use of these volatile plasticizers, while combining the properties of a low T_g, easily film-forming latex with a stabilizing high T_g component, is to use polymer blends, or structured lattices, such as core–shell particles. Core–shell particles can, for example, consist of a more hydrophobic core polymer formed from a high T_g polymer, surrounded by a more hydrophilic shell polymer composed of a low T_g polymer.

This paper compares the film-formation behavior of lattices with different particle structures and different core–shell morphologies.

2. Film formation of polymers

The film formation of lattices has been extensively studied. Dobler and Holl [1], Winnik [2] and Keddie [3] have reviewed the literature on latex film-formation. The following description of the film-formation process is a short summary of their findings. The film formation process for a system of monodisperse latex particles is commonly described in three stages:

2.1. Water evaporation, drying

Water evaporates first rapidly from the surface and forms a dry membrane at the surface [4]. The interstitial water

* Corresponding author. Tel.: +27-21-808-3172; fax: +27-21-808-4967.
E-mail addresses: rds@maties.sun.ac.za (R.D. Sanderson), mmein@maties.sun.ac.za (M. Meincken).

0032-3861/01/$ - see front matter
PII: S0032-3861(02)00346-4

subsequently evaporates more slowly, by diffusion through this membrane [4–7] and the drying front moves from the edges of the film, inwards [8]. Capillary forces caused by water evaporation create a nucleus of a two-dimensional ordered array [9]. Evaporation from the ordered area leads to a convective particle flux to the edges of the growing nucleus. Water is drawn from the surrounding regions to maintain the water level and to compensate for the evaporative water loss. This flux transports particles that subsequently become part of the ordered array, until finally the entire latex forms an ordered array in the form of a FCC colloidal crystal [10,11].

2.2. Particle deformation, coalescence

The latex surface flattens with further evaporation of the interstitial water. The spherical particles move closer to each other and are deformed into hexagons. The interfacial tension between polymer and water/air is sufficient to cause gradual coalescence. The observable particle boundaries are deformed and start to disappear [12]. Several hypotheses to account for the origin of the deforming forces have been proposed [1,13–19]. All of them describe the deformation forces acting as a function of the inverse particle radius. This means that the ability to form a film is greater for small particles than for large particles.

The particles are not only deformed into hexagons. Atomic force microscopy (AFM) studies [20–22] show that the surface is also smoothed, which means the particles are flattened.

Goudy et al. [23] found that the peak-to-valley height decreases at a greater rate for small particles than for large particles. This could be due to a greater driving force from capillarity in the smaller particles.

2.3. Particle interdiffusion

Physical contact between latex particles is insufficient to produce a strong continuous film. To obtain a stable film it is necessary that segments of polymer chains diffuse from one latex particle to another, to provide a sufficient level of entanglement between chains in neighboring latex particles, thus imparting mechanical strength. Increasing molecular weight and increasing incompatibility of polymers lower the interdiffusion rate.

The model developed by Dillon et al. [13] postulates that surface forces, such as surface tension, drive the polymer particles to coalesce. They applied the model developed by Frenkel [24] to describe the coalescence of spheres by viscous flow; as coalescence proceeds, the contact angle θ increases. This effect depends on the inverse particle radius r.

Brown's theory suggests that the capillary forces are the main driving forces for particle coalescence. Although different in mechanism, both proposed models—Brown's and Dillon's—suggest that small particles should coalesce more easily than large ones.

3. Core–shell polymers

Core–shell particles can offer the same advantage as homogeneous particles post-added with a film forming (coalescent) aid and avoid the disadvantage of solvent emission during the film-formation process. The low T_g shells lead to film formation while hard cores improve mechanical properties and stabilize the film.

Minimum film formation temperature (MFFT) measurements performed by Morgan [25] indicate that the shell has a greater impact on film formation than the core. The MFFT was observed to decrease with increasing thickness of the soft shell.

Juhue and Lang [26] studied the interdiffusion rate during the film formation of core–shell latex particles. Particles with a high T_g core and a low T_g shell exhibited interparticle chain diffusion that is comparable to what is found in the high T_g latex with an added film-forming solvent.

Lang and Perez [27] studied the flattening of PBMA and PMMA particles as well as the flattening of core–shell particles with a soft core surrounded by a hard shell by surface roughness measurements with the AFM. The results indicate that the polymer chain diffusion is not the predominant parameter in the surface film flattening but that the main driving force is rather the polymer-air surface tension, as also suggested in Ref. [28].

4. Experimental

Polymer lattices with different structures, different particle sizes and different core–shell ratios were investigated by AFM and their film-formation behavior compared.

4.1. Preparation of core–shell lattices

Synthesis of the core–shell lattices was conducted under flooded conditions, using reflux to exclude oxygen during the polymerization process. Typically, a reactor containing water (distilled and de-ionized quality), surfactant and ammonium carbonate as buffer was heated to 85 °C in a water bath equipped with a thermostat. Monomers, constituting the core phase, were then added over a period of 2 h. The shell-phase monomers were added subsequently, also over a period of 2 h. The composition of the monomers is described below.

After monomer addition the reactor was kept at 85 °C for a further 30 min before lowering the temperature. At a temperature of 70 °C *tert*-butyl hydroperoxide was added to react with any unreacted monomer still present in the

system. The reactor was then kept at 70 °C for 10 min before cooling to room temperature.

The theoretical value of the glass transition temperatures of the core and the shell were calculated by using the Fox equation [29]:

$$1/T_{g(copolymer)} = w_1/T_{g1} + \cdots + w_i/T_{gi} \quad (1)$$

In this equation T_{gi} is the glass transition of the constituent monomer's homopolymer and w_i is the weight fraction of that particular monomer in the copolymer composition.

4.2. Preparation of gradient lattices

The preparation of the reactor was the same as for the core–shell synthesis. The gradient particles consisted of a core surrounded by a shell with gradually changing composition. Synthesis of the gradient latex was achieved by separating the monomers that constitute the 'hard' part of the latex, such as methylmethacrylate (MMA) and styrene (S), from the monomers that constitute the 'soft' part of the latex, such as butyl acrylate (BA). The reaction was initiated by adding the solution of 'hard' monomers over a period of 15 min into the reactor to 'seed' the emulsion polymerization reaction before starting the second addition of 'soft' monomer, not to the reactor, but to the tank containing the 'hard' monomers.

In this way the composition of the monomers in the tank metered into the reactor was constantly changed and the glass transition of the resulting polymers changed gradually accordingly. The result of this synthesis was a latex particle with a structure that changes gradually from a hard polymer core phase to a soft outer shell phase.

Polymer films were prepared by spreading a thin layer of the polymer emulsion on a silicon surface, followed by thinning and flattening with a microscope slide. The thickness of these films was about 50 μm.

4.3. Investigated emulsions

Different lattices were prepared by emulsion polymerization to compare lattices on a preferably wide field of investigation.

To compare *different polymer structures*, the following emulsions, all containing the same monomers, were produced:

- A latex containing conventional particles with 57% S, 40% BA, and 3% methacrylic acid (MAA). The theoretical T_g (from Eq. (1)) was 19.22 °C. The average particle diameter, as measured with photon correlation spectroscopy (PCS), was 102.1 nm.
- A latex containing core–shell particles with 69% S, 24% BA, and 7% MAA in the core and 49% S, 49% BA and 2% MAA in the shell. The theoretical T_g of the core was 49.95 °C, and the theoretical T_g of the shell 5.1 °C. The average particle diameter obtained by PCS was 88 nm.
- A latex containing core–shell particles with a crosslinked core. The crosslinking was achieved using ethylene glycol dimethacrylate (EGDMA); the monomers were the same as for the previous core–shell polymer. The theoretical T_g of the core was 65.5 °C, and the theoretical T_g of the shell 5.1 °C. The average particle diameter obtained by PCS was 85.7 nm.
- A latex with gradient particles with core–shell structure. The core consisted of 69% S, 24% BA, and 7% MAA and had a theoretical T_g of 49.95 °C. The shell consisted of 49% S, 49% BA and 2% MAA gradually changing from pure PS and MAA at the inside to pure BA outside. Therefore the theoretical T_g of the outer part of the shell is −54 °C and around 100 °C at the inner part surrounding the core. The average particle diameter obtained by PCS was 104.7 nm.

To compare *different core–shell ratios*, core–shell particles with a crosslinked core, as described earlier, were produced with core/shell ratios (by mass) of 2/3, 2/4, etc. to 2/8. The average particle sizes obtained by PCS varied slightly, from 100 to 110 nm.

To obtain *different particle sizes*, core–shell particles with a crosslinked core and a core–shell ratio of 2/5 were produced with different surfactants (anionic surfactants from Stepan Company, Northfield, IL, USA). The monomers used were the same as before. The theoretical T_g of the core was 89.93 °C and the theoretical T_g of the shell was 6.16 °C.

The following surfactants resulted in the following particle sizes:

- Polystep B25, a sodium salt of a sulfated alkyl alcohol. The obtained particle size was 68.5 nm.
- Polystep B27, a sodium salt of nonylphenoxypolyethyleneoxyethanol sulfate. The obtained particle size was 79 nm.
- Polystep B29, a sodium salt of a sulfated alkyl alcohol. The obtained particle size was 322 nm.
- A blend of 25% B27 and 75% B29. The obtained particle size was 105 nm.
- A blend of 15% B27 and 85% B29. The obtained particle size was 110 nm.

4.4. Analysis by atomic force microscopy

AFM consists basically of a sharp silicon tip mounted on a cantilever that is scanned across a sample surface and the forces acting between the tip and the surface are detected. An electronic feedback loop controls the system, so that the force can be kept constant. From this electronic feedback signal a three-dimensional image of the topography can be calculated.

In the non-contact mode, for example, the change of resonance frequency or amplitude of the oscillating cantilever is detected.

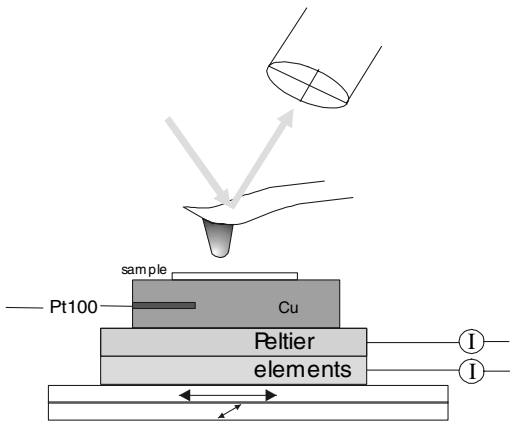

Fig. 1. The experimental setup used for the AFM experiments. The polymer sample is placed on a heating/cooling stage, which is located on a *x*/*y* translator. The AFM is placed above the sample. The temperature sensor (PT100) is mounted in the copper base plate.

The experimental setup used is shown in Fig. 1. The sample to be analyzed was placed on a heating/cooling stage, consisting of two serial Peltier elements. The temperature could be varied from −20 to 120 °C. The AFM was placed above the sample and images were acquired at different temperatures or at a constant temperature as a function of time.

The AFM, a Topometrix Explorer, was operated in the stationary, low-amplitude, non-contact mode. The resonance frequency of the low frequency, non-contact silicon cantilevers (Nanosensors GmbH) was about 170 kHz. The cantilever was driven at its resonance frequency with a driving-amplitude of 0.2 mV. The measurements were performed under ambient conditions.

The piezo scanner was not specially shielded from the heat. Measurements conducted on a calibration grid showed that the scanner calibration did not change with temperature in the applied temperature range.

AFM images of the polymer film were acquired every 30 min after casting the film. A typical sequence of the acquired AFM images is shown in Fig. 2. Once the film had dried, the time between the acquisition of two images was increased to a few hours. The average particle diameter of the latex spheres and the standard deviation were calculated for each AFM image. Unlike other studies Ref. [27], in which the surface roughness is observed as a parameter to follow the film formation here the particle diameter was chosen as a monitoring parameter for the film formation. Studying only the surface roughness of the polymer does not take into account that the particles deform not uniform, but grow protrusions before they diffuse.

The average particle diameter was determined by using the Topometrix imaging software. Line scans were drawn through the image and the peak-to-peak (or valley-to-valley) distances measured. This was done for all recognizable particles in the image from different directions and resulted in an average particle diameter with a standard deviation.

The resulting curves show the average particle diameter as a function of time or temperature. These curves display the deformation behavior of the particles and show the different film-formation kinetics of the lattices.

To be able to compare the acquired values of the different polymers, the average diameter of the first AFM image was set to be 100% and the following particle sizes were calculated accordingly, to visualize changes in the particle size with time or temperature. An increase to 300% or more did not necessarily mean that the diameter of one particle increased that much, but rather that the particles started to coagulate and interdiffuse. In this case two, or more particles might be coalesced and appear as one big particle. In the case of the core–shell particles the core diameter was plotted as soon as the cores became visible at the surface. This resulted in values smaller than 100% for the average particle diameter. Fig. 3 shows a sequence of AFM images where the cores have been revealed.

4.5. MFFT measurements

The MFFT is described as the minimum temperature at which a water-borne synthetic latex or emulsion will coalesce when cast as a thin film. The MFFT is closely related to T_g but not synonymous with it. Above the MFFT the latex will form a clear, transparent film. Below the MFFT a white powdery, cracked film is formed.

The minimum film formation temperature is measured with a MFFT bar. This bar consists of a metal plate, which is electronically heated/cooled over a temperature gradient in a known temperature range (e.g. from −5 to 13 °C), so that the one end is cooler than the other end. Air or nitrogen is caused to flow constantly over the surface, from the cool end to the warm end, to dry the thin film. The MFFT is the temperature at which the film changes from a white, cracked film into a transparent film.

For low T_g polymers with a T_g close to 0 °C it is hardly possible to determine the MFFT, because the latex is freezing instead of film-forming in the temperature range of interest. All core–shell particles investigated in this study had low T_g shells with a shell T_g of about 2 °C and in all cases it was not possible to determine a MFFT value.

The MFFT of the conventional unstructured latex was 19 °C.

5. Results and discussion

Figs. 3 and 4 show typical image sequences of deforming structured latex particles. It can be seen how the shells begin to deform, coagulate and interdiffuse. The cores only become visible once the shell polymer formed a flat, smooth film around the core particles, until then they are covered with shell polymer. In the case of the core–shell particles in Fig. 4 the cores were crosslinked and did not flow; they remained in a spherical shape even at high

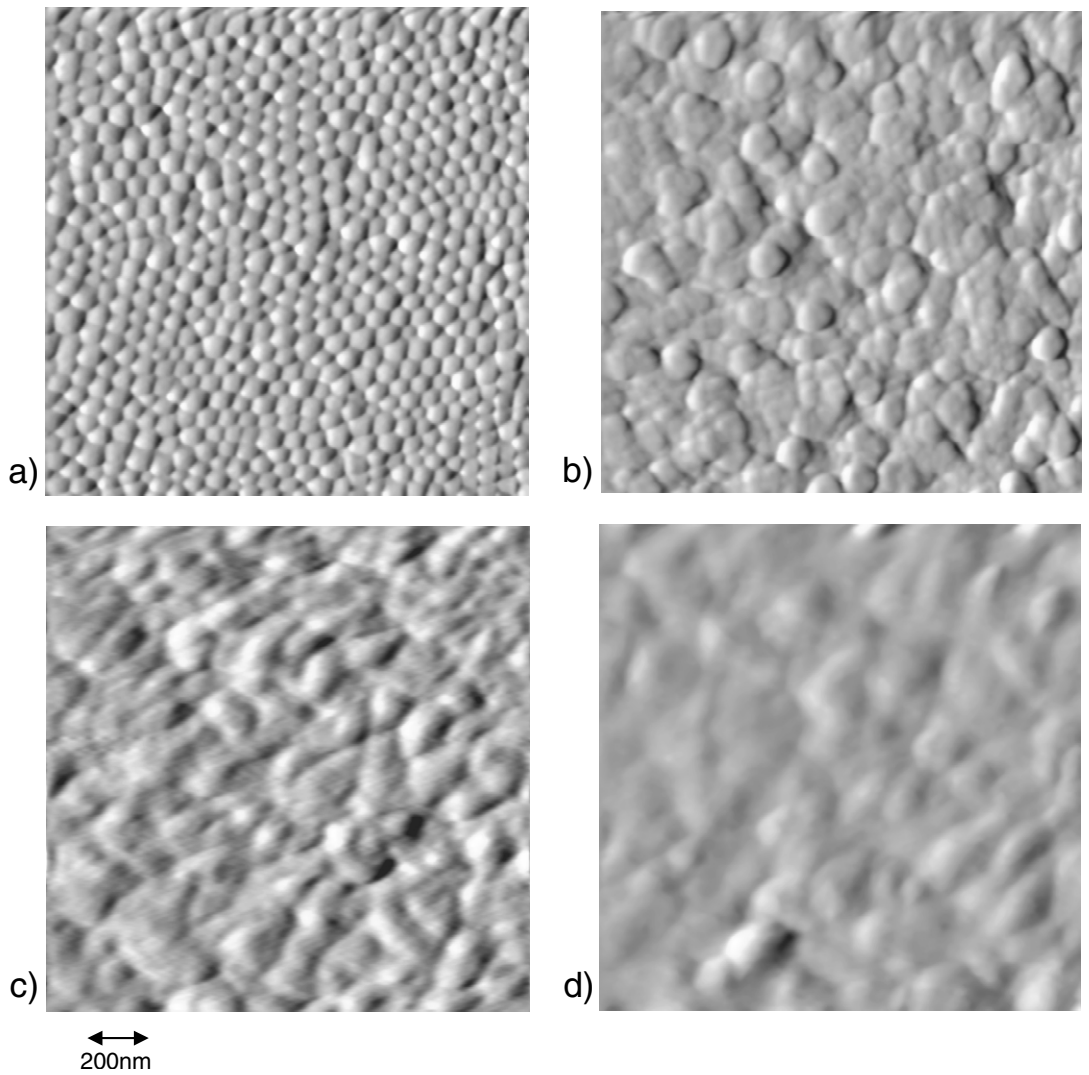

Fig. 2. A typical sequence of AFM images of an unstructured latex with a T_g of about 19 °C. The images were acquired 30, 240, 660 and 1440 min after the polymer film was cast.

temperatures, whereas the uncrosslinked core particles in Fig. 3 first appear at the surface but then start to flow at temperatures above the T_g and form a smooth film with further increasing temperature.

Lattices with unstructured particles, core–shell particles, core–shell particles with crosslinked core and gradient core–shell particles were investigated and their film formation behaviors compared. All particles contained the same monomers and had roughly the same particle size of 90–100 nm.

Fig. 5 shows the increase in average particle diameter as a function of time for the different particle structures. The two core–shell lattices follow the same trend. Their particle diameters increase faster than the average diameter of the conventional, or the gradient particles. This means that the particles coalesced earlier and the film formation started earlier. This is to be expected, since the soft shells have a T_g well below room temperature and thus will start flowing and coalescing earlier at room temperature. The T_g of the conventional latex is only slightly below room temperature, which means that the polymers cannot flow as easily as the shell polymers of the core–shell latex and that the film formation process takes place over a longer time.

The diameter of the gradient particles remains almost constant after an initial decrease. The soft butyl acrylate part of the shell started flowing around the remaining parts consisting of the cores surrounded by the harder polymer phase at room temperature. The T_g of the harder polymer phase at the inner part of the shell is substantially higher than room temperature, so the remaining shell of the polymer could not flow and the particle diameter remained constant with time.

A latex consisting of core–shell particles with a hard core and a soft shell that film-forms easily at room temperature is obviously the favored polymer structure, if film formation under ambient conditions is desired.

Fig. 6 shows the average particle diameter of differently structured particles as a function of temperature. The

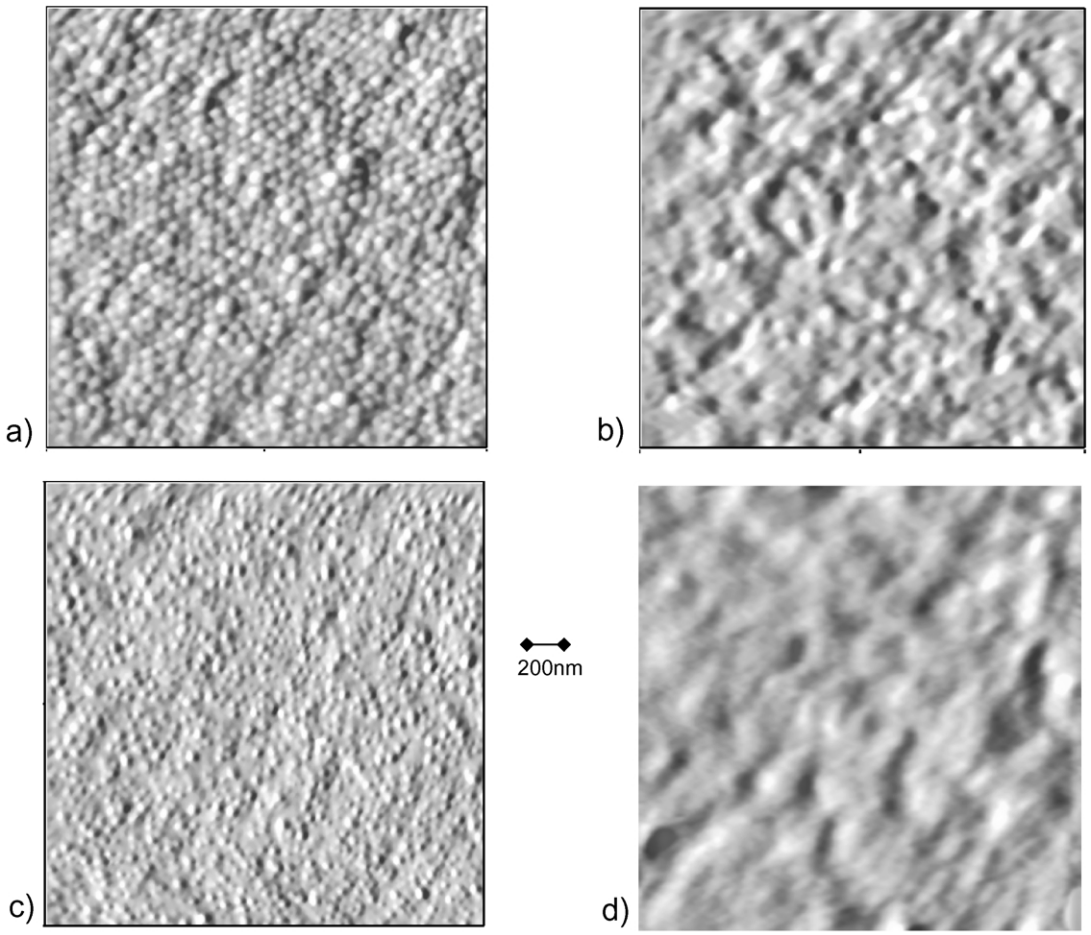

Fig. 3. A typical sequence of AFM images of a core–shell latex with uncrosslinked cores. The images were acquired at temperatures of (a) 2 °C, (b) 30 °C, (c) 42 °C and (d) 80 °C.

temperature at which the particle diameter starts to increase can be regarded as the glass transition temperature. These temperatures are marked with an arrow in Fig. 6. At this temperature, the polymeric chains can start to flow and the particles grow larger. In the case of the core–shell particles it is even possible to determine the T_g of the core, which is not possible with common methods like differential scanning calorimetry (DSC) or dynamic mechanic analysis (DMA), as they only measure an average T_g value of the entire sample. Once the cores become visible at the surface, their average particle diameter is plotted in the temperature/diameter graph.

For the unstructured latex the determined T_g is about 18 °C. The shells of both core–shell lattices start to flow below 5 °C. The cores of the core–shell particles start to flow above their T_g of about 48 °C, while the crosslinked cores of the second core–shell latex remain at their original size. For the gradient particles it is not possible to determine a shell T_g, since the shell structure varies gradually, from the inside to outside, in the amount of hard and soft polymer. The T_g of the harder polymer phase is well above room temperature, which means that the inner parts of the shell cannot flow at temperatures below the T_g of the hard polymer phase, and thus the particle diameter remains more or less constant.

To observe the influence of the core/shell ratio on the film-formation process, core–shell lattices with a crosslinked core and different core/shell ratios were prepared. The composition was the same for all compared polymers, and the core/shell ratio was altered from 2/3 to 2/8. Fig. 7 shows the results.

Morgan [25] studied the film-formation behavior of different core–shell particles with a soft shell surrounding a hard, but uncrosslinked, core for different core/shell ratios. They found that with increasing thickness of the soft shell the MFFT decreased, since the film-forming abilities were increased.

Our measurements could not confirm this finding. All latex samples behaved very similarly in the way they deformed. All curves followed the same trend, meaning that there was no difference in the particle deformation or the coalescence behavior. The soft shell started deforming and flowing at room temperature and caused the increase in particle diameter.

The lattices with the core/shell ratio of 2/3 and 2/4 have larger cores than the other lattices with smaller core/shell

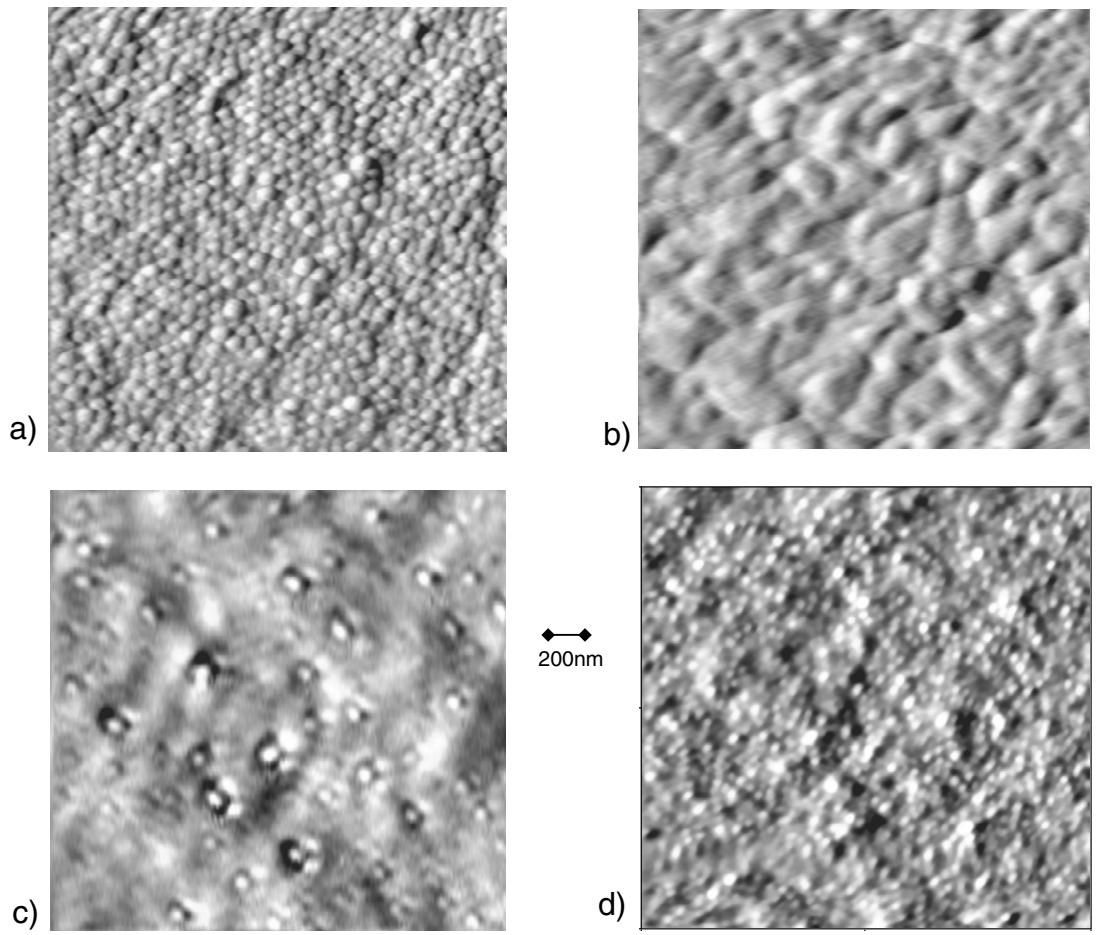

Fig. 4. A typical sequence of AFM images of a core–shell latex with crosslinked cores. The images were acquired at temperatures of (a) 2 °C, (b) 25 °C, (c) 40 °C and (d) 80 °C.

ratios, covered only with a comparatively thin shell. After about 2 h the cores were revealed at the surface surrounded by shell polymers that form a film around the cores. The particle size of the cores did not increase with time because of the crosslinking. For the polymers with thicker shells, the shells were only deformed with time and started to coalesce, but the cores did not become visible at the surface.

If a smooth surface is desired then the core/shell ratio

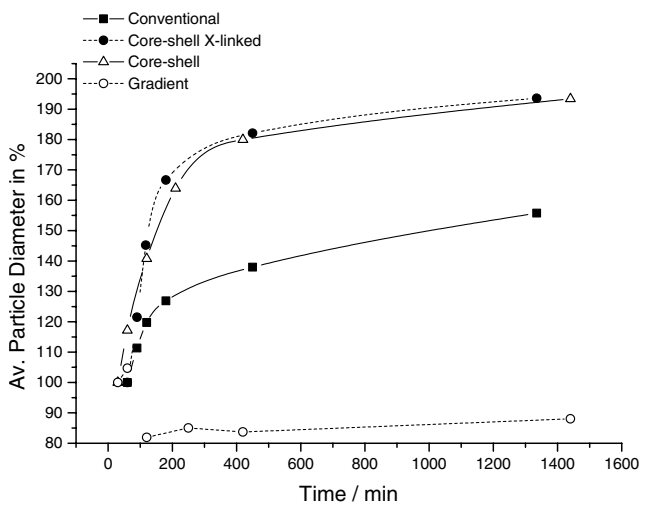

Fig. 5. Increase in the average particle diameter as a function of time for different polymer structures: conventional particles, core–shell particles with crosslinked core, core–shell particles and gradient particles.

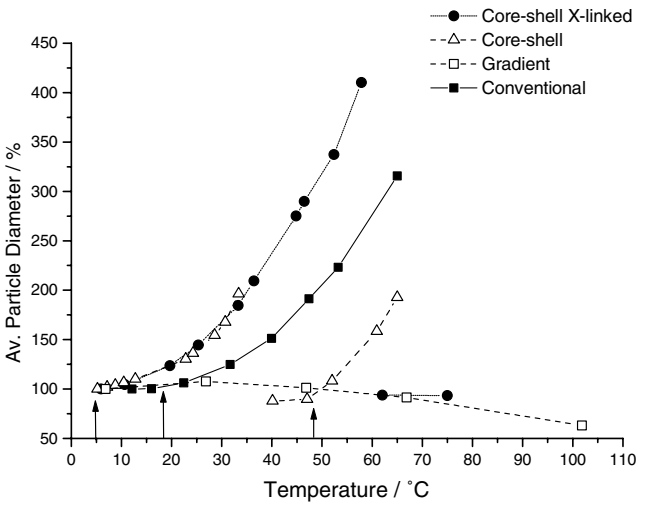

Fig. 6. Increase in the average particle diameter as a function of temperature for different polymer structures: conventional particles, core–shell particles with crosslinked core, core–shell particles and gradient particles.

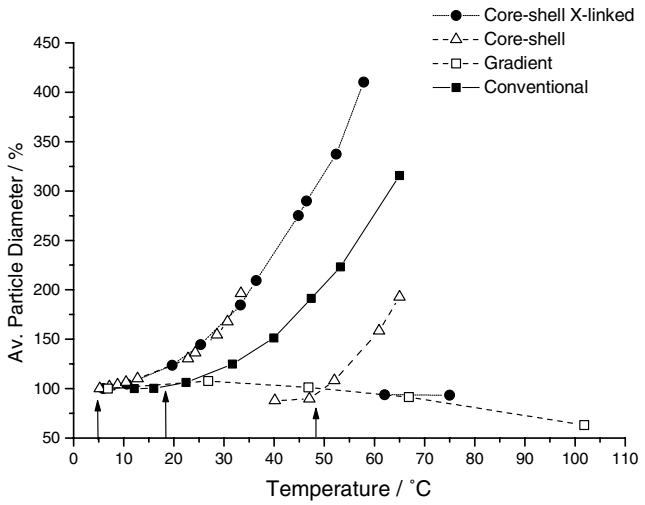

Fig. 7. Increase in the average particle diameter as a function of time for core–shell lattices with different core/shell ratios, ranging from 2/3 to 2/8.

should obviously be rather small. For the polymer composition used here, a core/shell ratio of 2/5 or smaller was found to be sufficient to achieve a smooth film surface.

Core–shell particles with a crosslinked core and particle diameters ranging from 69 to 320 nm were prepared to investigate the influence of the particle size on the film-formation.

The time dependent growth behavior of the polymer particles shows a clear relation to the particle size, as shown in Fig. 8. It is clearly visible that the smaller particles were sooner deformed to a larger extent and flowed more easily than the larger particles.

According to the theories of Dillon [13] and Brown [9], our experimental results show that the smaller particles coalesced more easily than the larger ones and that the deforming forces were larger for the smaller particles. This confirms the theory of Kendall and Padget [18], that the deforming force is inversely proportional to the particle radius. It also confirms the findings of Jensen and Morgan [19] that the MFFT increases with the particle diameter—meaning that the ability to form a film decreases with increasing particle size.

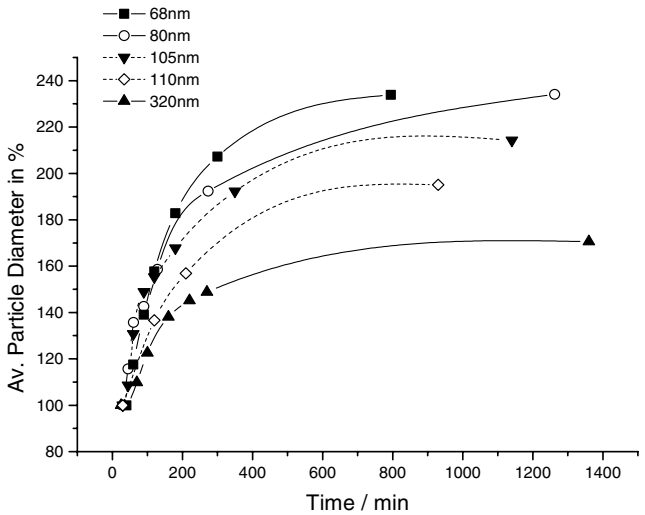

Fig. 8. Increase in the average particle diameter as a function of time for core–shell lattices with a core/shell ratio of 2/5 and particle sizes of 68, 80, 105, 110 and 320 nm.

Since the lattices with different core/shell ratios and different particle sizes were all of the same composition, the curves of the average particle diameter as a function of temperature did not give much additional information. All shells started to deform at the same temperature and the curves then followed the same trend.

6. Conclusions

The deformation and film-formation behavior of different polymer particles were investigated by AFM. To achieve a comprehensive picture of the film formation of latex particles, lattices with different particle structures, different core–shell ratios and different particle sizes were studied.

A comparison of different particle structures with the same particle size and the same monomers showed that core–shell particles with a hard core and a soft shell film-form faster than, for example, conventional unstructured particles do. This is due to the low T_g shell polymer surrounding the harder core that can flow and coalesce under ambient conditions. Plotting the average particle diameter as a function of temperature allows the determination of the temperature region of the T_g of the latex particles. T_g is the temperature at which the particles can start to flow and deform. In the graph this is the temperature at which the average particle diameter starts to increase. With the AFM it is even possible to determine individual T_gs for different polymer phases in structured polymers, as in core shell polymers, if the core is not crosslinked and can, like the shell, start to flow. This is not possible with common methods such as DSC or DMA, which measure only an average T_g value for the entire sample.

The effect of the shell thickness of core–shell particles found by MFFT measurements by Morgan [25], could not be confirmed by AFM measurements. In the present study it was found that the polymers with different core–shell ratios behave very similarly, up to a critical core/shell ratio. If the shell is too thin, as for the core/shell ratios 2/3 and 2/4, the core is revealed at the surface after a certain time, which leads to a higher surface corrugation. The different findings can be explained by the different techniques used: MFFT measurements yield information about the bulk properties, while the AFM is purely a surface analysis instrument. Only the top layers of the polymers are imaged and the polymer structure of the bulk is not necessarily the same near as the surface; here the segmental distribution of polymer chains might differ significantly. Most theories, concerning the different structure of a polymer close to the surface, [30–34] predict a lowering of the T_g at the surface [35], due to the

excess of chain ends close to the free surface, and therewith an enhanced film-forming ability. This effect might dominate the dependence of T_g on the shell thickness, which could therefore not be observed with the AFM.

The theoretical model of particle coalescence proposed by Kendall and Padget [18] was confirmed experimentally. A strong dependency of the film formation behavior on the particle size was found. Smaller particles deform to a greater extent and coalesce faster than larger particles. This is also in good agreement with the theory of Brown [9], Kendall and Padget, and to the experimental results obtained by Jensen and Morgan [19], Kan [20], Goh [22], and Goudy [23].

Acknowledgments

The Plascon Research Center supplied the investigated lattices. Dr Deon de Wet-Roos and John Engelbrecht of Plascon Research supported the project with their valuable advice. Funding was provided by Plascon, the National Research Foundation (NRF) and the Technology and Human Resources for Industry Program (THRIP) of South Africa.

References

[1] Dobler F, Holl Y. Trends Polym Sci 1996;4:145.
[2] Winnik M. Emulsion polymerization and emulsion polymers. New York: Wiley; 1997.
[3] Keddie J. Mater Sci 1997;9:101.
[4] Sheetz D. J Appl Polym Sci 1965;9:3759.
[5] Vanderhoff J, Bradford E, Carrington W. J Polym Sci: Symp 1973;41:155.
[6] Croll S. J Coat Technol 1986;58:41.
[7] Croll S. J Coat Technol 1987;59:81.
[8] Winnik M, Feng J. J Coat Technol 1996;68:39.
[9] Brown G. J Polym Sci 1956;22:423.
[10] Pusey P, van Megen W, Bartlett P. Phys Rev Lett 1989;63:2753.
[11] Rieger J, Haedicke E, Lindner P. Phys Rev Lett 1992;68:2782.
[12] El-Aasser S, Robertson A. J Paint Technol 1975;47:50.
[13] Dillon R, Matheson L, Bradford E. J Colloid Sci 1951;6:108.
[14] Vanderhoff J, Tarkowski H, Jenkins M, Bradford E. J Macromol Chem 1966;1:361.
[15] Sperry P, Snyder B, O'Dowd M, Lesko P. Langmuir 1994;10:2619.
[16] Eckersley S, Rudin A. J Appl Polym Sci 1994;53:1139.
[17] Vanderhoff J. Br Polym J 1970;2:161.
[18] Kendall K, Padget J. Int J Adhesion Adhesives 1982;July:149.
[19] Jensen D, Morgan L. J Appl Polym Sci 1991;42:2845.
[20] Kan C. Proceedings TAPPI Adv. Coating Foundation Symposium; 1993. p. 101.
[21] Lin F, Meier D. Langmuir 1995;11:2726.
[22] Goh C, Juhue D, Leung O, Wang Y, Winnik M. Langmuir 1993;9:1319.
[23] Goudy A, Gee M, Biggs S, Underwood S. Langmuir 1995;11:4454.
[24] Frenkel J. J Phys 1945;9:385.
[25] Morgan L. J Appl Polym Sci 1982;27:2033.
[26] Juhue D, Lang J. Macromolecules 1995;28:1306.
[27] Perez E, Lang J. Langmuir 2000;16:1874.
[28] Perez E, Lang J. Macromolecules 1999;32:1626.
[29] Mark H, Bikales N, Overberger C, Menges G. Encyclopedia of polymer science and engineering, 2nd ed. John Wiley & Sons, Inc. USA. 1985.
[30] Mayes A. Macromolecules 1994;27:3114.
[31] de Gennes P. C R Acad Sci (Paris) 1988;307:1841.
[32] Tanaka K, Takahara A, Kajiyama T. Macromolecules 1996;29:3232.
[33] Kajiyama T, Tanaka K, Takahara A. Macromolecules 1997;30:280.
[34] Forrest J, Dalnoki-Veress K, Dutcher J. Phys Rev E 1997;56:5705.
[35] Wu W, Satija S, Majkrazak C. Polym Commun 1991;32:262.